Electronic Supplementary Material (ESI) for Journal of Materials Chemistry C.

Supporting Information for

Double Peak Emission in Lead Halide Perovskites by Self-Absorption

Konstantin Schötz[1], Abdelrahman Askar[2], Wei Peng[3], Dominik Seeberger[4], Tanaji P. Guijar[4], Mukundan Thelakkat[4], Anna Köhler[1,5], Sven Hüttner[4], Osman M. Bakr[3], Karthik Shankar[2], Fabian Panzer[1*]

[1]: Soft Matter Optoelectronics, University of Bayreuth, 95440 Bayreuth, Germany

[2]: Department of Electrical and Computer Engineering, University of Alberta, Edmonton, AB T6G 1H9, Canada

[3]: King Abdullah University of Science and Technology (KAUST), Division of Physical Sciences and Engineering, Thuwal23955-6900, Kingdom of Saudi Arabia

[4]: Department of Chemistry, University of Bayreuth, 95440 Bayreuth, Germany

[5]: Bayreuth Institute of Macromolecular Research (BIMF) and Bavarian Polymer Institute (BPI), University of Bayreuth, 95440 Bayreuth, Germany.

Corresponding Author: fabian.panzer@uni-bayreuth.de

1. Logarithmic version of Figure 1a

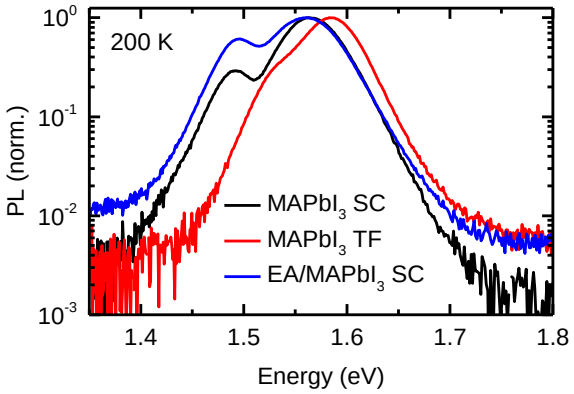

Figure S1: Logarithmic plot of the PL of the iodine samples at 200 K from Figure 1 in the main text. In the logarithmic depiction of the PL of the $MAPbI_3$ thin film, the additional shoulder at 1.53 eV becomes more obvious.

2. PL Peak 2 intensity dependence on excitation laser spot

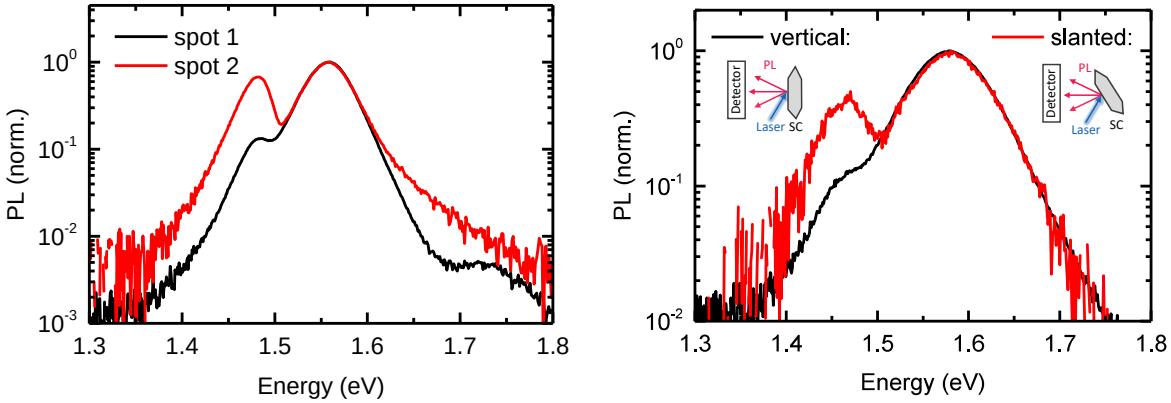

Figure S2: Left: Normalized PL of a $MAPbI_3$ single crystal at 170 K. Between both measurements the spot of the excitation laser was moved in such a way that at the first position, Peak 2 was less pronounced (spot 1, black curve), while for the second position, Peak 2 was strongly pronounced (spot 2, red curve). Right: Normalized PL of a $MAPbI_3$ single crystal at 300 K under vertical detection (black) and slanted detection (red) as illustrated in the inset.

3. Temperature-dependent PL of other perovskite samples

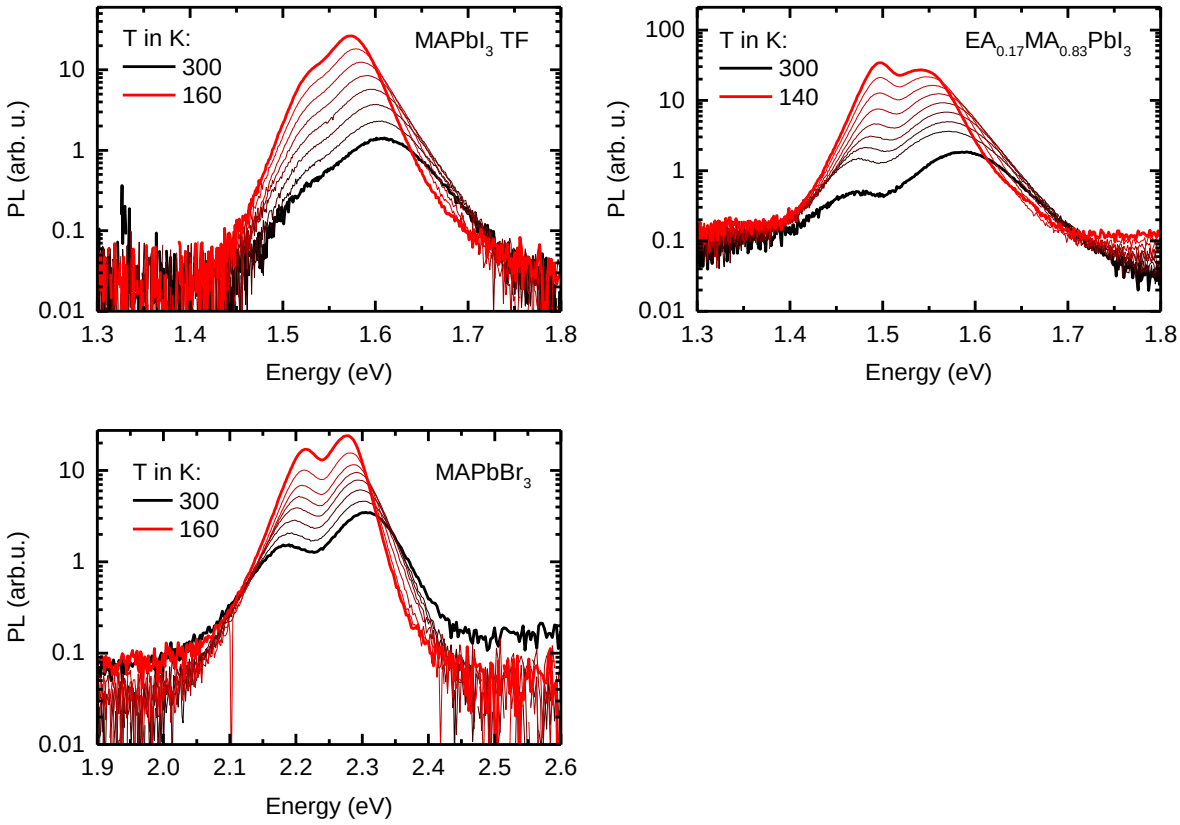

Figure S3: Temperature-dependent PL of the $MAPbI_3$ thin film (TF), the $EA_{0.17}MA_{0.83}PbI_3$ single crystal and the $MAPbBr_3$ single crystal. The temperature difference between each line is 20 K.

4. Spectral decomposition of measured PL spectrum

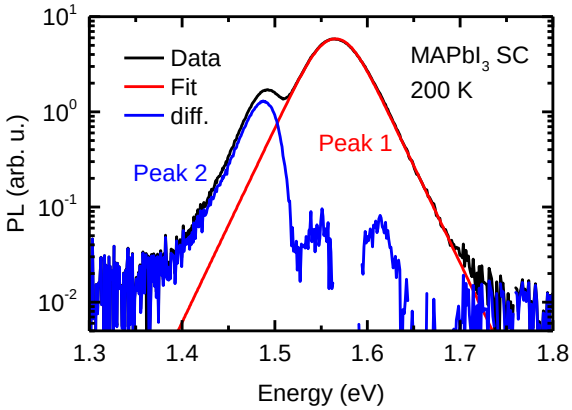

Figure S4: Decomposition of the PL spectrum of the $MAPbI_3$ single crystal at 200 K. The experimental data is shown in black. The red curve presents an empiric fit to Peak 1 using two hyperbolic secants with equal intensity and width, but shifted by 14 meV to obtain a better fit. The difference between fit and data is plotted in blue and presents the shape of Peak 2.

5. PL of the $MAPbI_3$ single crystal between 160 – 120 K

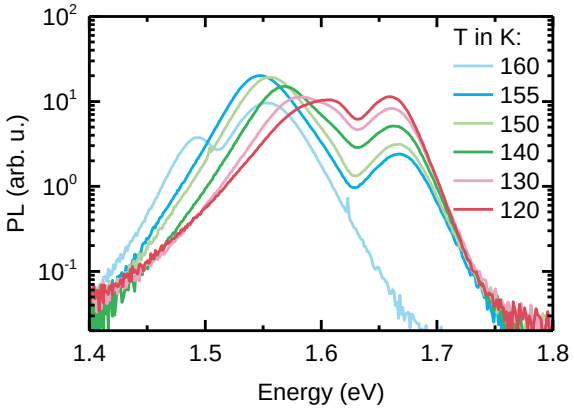

Figure S5: PL spectra of the $MAPbI_3$ single crystal in the phase transition region between 160 K and 120 K.

6. Low-temperature PL of the $MAPbI_3$ single crystal

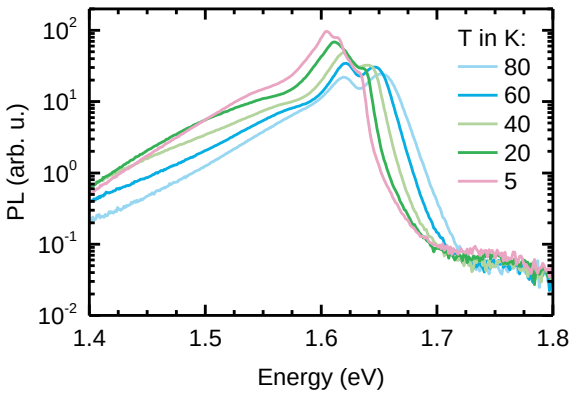

Figure S6: Temperature-dependent PL of the $MAPbI_3$ single crystal in the range between 80 K to 5 K.

7. Verification of different extend of strain in the $MAPbI_3$ films on PET- and glass substrate

As mentioned in the main text, strain in the sample has influence on the phase transition of the perovskite. The quantification of the tetragonal to orthorhombic phase transition of the $MAPbI_3$ thin films on PET and glass substrate via their absorption spectra (see Figure S7a,b) was performed identical to the method described in in the work by Meier et al. and Panzer et al..[1-2] We extracted the optical density (OD) of the films at 1.62 eV from 170 K to 100 K (Figure S7c). As only the tetragonal phase absorbs at this energy in this temperature range, the OD value is representative of the amount of tetragonal phase in the system. We then calculated the derivative of the temperature dependent OD and fitted this with a Gaussian function (Figure S7d), where its center is the critical temperature T_c and its full width at half maximum (FWHM) describes the width of the phase transition. By doing so, we obtain for the film on the glass substrate $T_{c,Glass}$ = 145.9 ± 0.3 K, $FWHM_{Glass}$ = 10.1 ± 0.7 K and for the PET substrate $T_{c,PET}$ = 147.2 ± 0.2 K, $FWHM_{PET}$ = 8.8 ± 0.6 K.

Additionally, strain in the sample should have influence on the lattice constants and thus on the PL peak position. We therefore analyzed the temperature-dependence of the PL peak position of the $MAPbI_3$ films on PET and glass substrate (see Figure S7e), where we find a shift of 0.25 meV/K for the sample on glass, and 0.28 meV/K for the sample on PET. The reduced shift for the sample on glass is consistent with more strain being present that counteracts the decrease of the lattice constant of $MAPbI_3$ upon cooling. This leads to a decreased temperature depend band gap shift, which is reflected in the PL position.

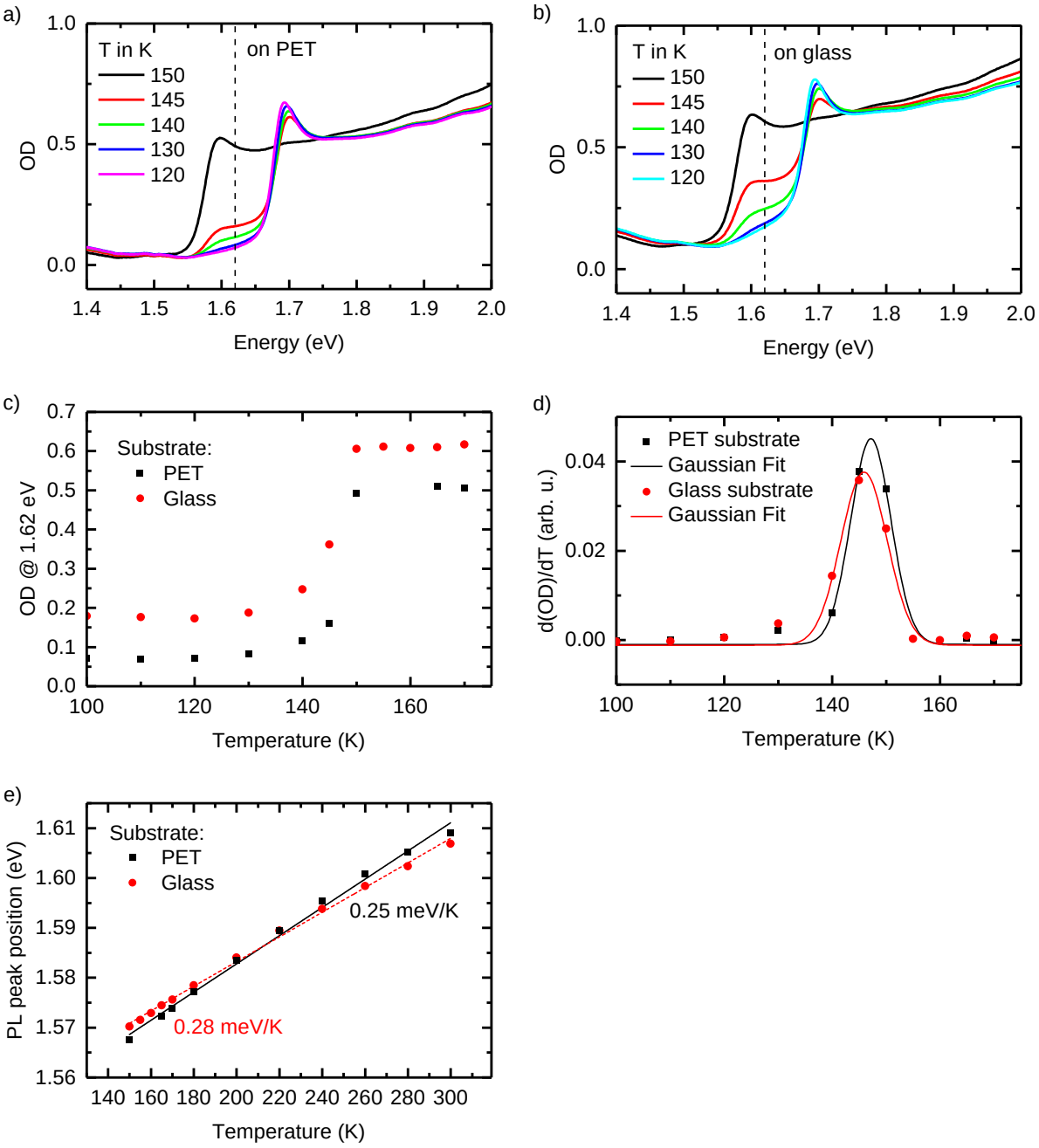

Figure S7: Temperature-dependent absorption of a $MAPbI_3$ thin film on (a) PET and (b) glass substrate. (c) Optical density of both films at 1.62 eV in the temperature range of the tetragonal to orthorhombic phase transition, i.e. 170 K to 100 K. (d) Derivative of the OD at 1.62 eV together with Gaussian fits (solid lines). (e) Temperature-dependence of the PL peak position of the $MAPbI_3$ films on PET (black squares) and glass substrate (red circles), together with linear fits to the data points.

8. Spectral decomposition of the PL of MAPbI3 film on glass and PET substrate

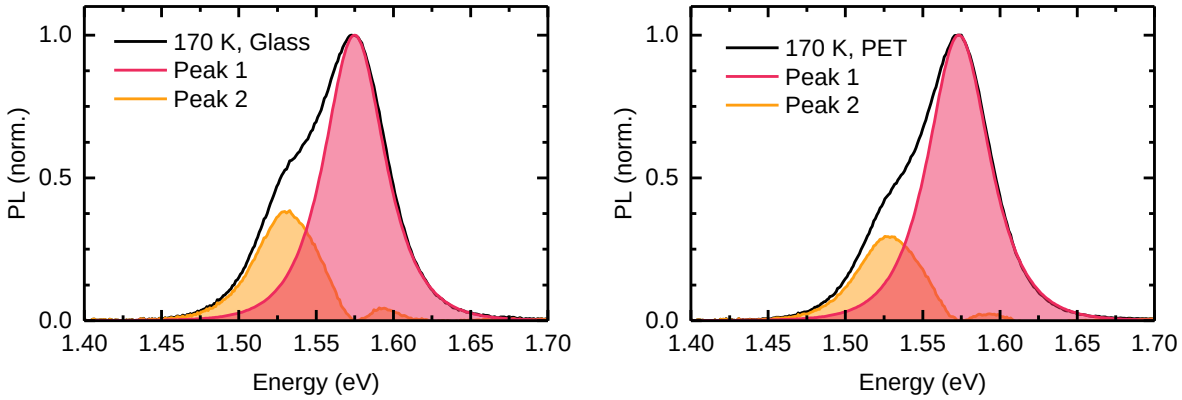

Figure S8: Spectral decomposition of the $MAPbI_3$ film on glass (left) and PET substrate (right) by fitting a hyperbolic secant to Peak 2

9. Discussion of the spectral blue shift upon passivation

A schematic illustration of the influence of surface passivation on the PL is shown in Figure S9. Before passivation, there is an increased defect density and consequently an increased non-radiative recombination rate near the surface of the perovskite (blue shaded area). Consequently, the PL intensity is reduced in the surface region and most of the detected PL comes from the inside of the material and thus is to a certain extend self-absorbed and therefore red-shifted compared to the intrinsic PL. Surface passivation reduces the defect density at the surface and consequently increases the PL intensity in this area. Hence, the detectable PL after passivation is on average less self-absorbed and less red-shifted than before passivation. Therefore, the PL after surface passivation occurs blue-shifted compared to the PL before passivation.

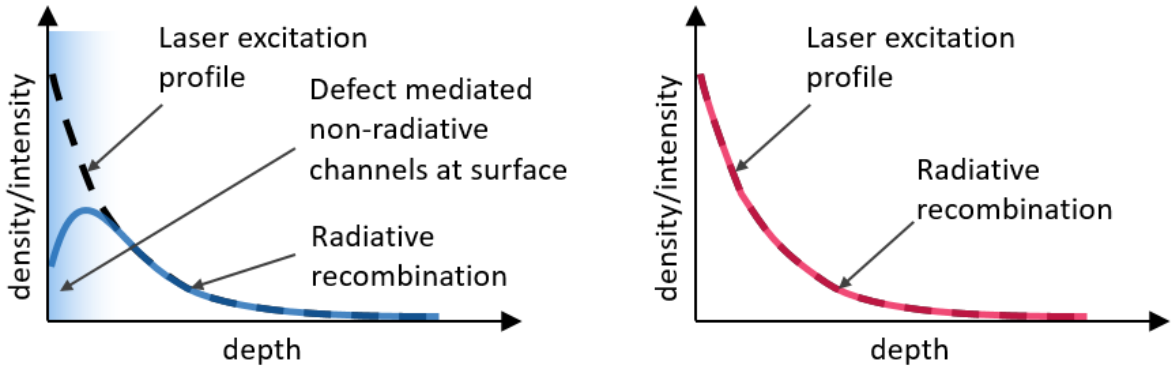

Figure S9: Schematic illustration of the PL intensity (solid line) as a function of depth after laser excitation (dashed line), before (left) and after surface passivation (right).

10. Estimation of charge carrier density after excitation

The initial charge carrier density $n_{initial}$ near the surface of the sample after laser excitation for very short laser pulses, can be estimated by the laser fluence H_e divided by the photon energy E_{photon}, times the absorption coefficient α:

$$n_{initial} = \frac{H_e}{E_{photon}} \alpha$$

With $E_{photon} = 3.67$ eV, $\alpha = 5 \cdot 10^5\ cm^{-1}$,[3] the lowest fluence $H_e = 10\ \frac{\mu J}{cm^2}$ used in this study corresponds to an initial charge carrier density $n_{initial}\left(10\ \frac{\mu J}{cm^2}\right) = 8.5 \cdot 10^{18}\ cm^{-3}$ and the highest fluence $H_e = 420\ \frac{\mu J}{cm^2}$ corresponds to an initial charge carrier density $n_{initial}\left(400\,\frac{\mu J}{cm^2}\right) = 3.6 \cdot 10^{20} cm^{-3}$. However, the sample is excited in a finite time, that is the pulse width $T_{pulse} = 3\ ns$ of the excitation laser. On this time scale also recombination processes need to be considered. Thus, the change of charge carrier density near the surface during excitation is given by

$$\frac{dn}{dt} = \frac{H_e}{E_{photon}\ T_{pulse}} \alpha - (k_1 n + k_2 n^2 + k_3 n^3)$$

With typical values for the rate constants, $k_1 = 10^6$, $k_2 = 6.8 \cdot 10^{-10}$ and $k_3 = 10^{-29}$,[3] we obtain for the lowest fluence $n\left(10\ \frac{\mu J}{cm^2}\right) = 2 \cdot 10^{18}\ cm^{-3}$ and for the highest fluence $n\left(400\,\frac{\mu J}{cm^2}\right) = 1.2 \cdot 10^{19}\ cm^{-3}$. We point out that this reflects only the charge carrier density near the surface and directly after laser excitation, so that the calculated values represent an upper limit.

Supporting References:

1. Meier, T.; Gujar, T. P.; Schönleber, A.; Olthof, S.; Meerholz, K.; van Smaalen, S.; Panzer, F.; Thelakkat, M.; Köhler, A., Impact of excess PbI_2 on the structure and the temperature dependent optical properties of methylammonium lead iodide perovskites. *J Mater Chem C* **2018,** *6* (28), 7512-7519.
2. Panzer, F.; Bössler, H.; Köhler, A., Temperature Induced Order-Disorder Transition in Solutions of Conjugated Polymers Probed by Optical Spectroscopy. *J Phys Chem Lett* **2017,** *8* (1), 114-125.
3. Crothers, T. W.; Milot, R. L.; Patel, J. B.; Parrott, E. S.; Schlipf, J.; Müller-Buschbaum, P.; Johnston, M. B.; Herz, L. M., Photon Reabsorption Masks Intrinsic Bimolecular Charge-Carrier Recombination in $CH_3NH_3PbI_3$ Perovskite. *Nano Lett* **2017,** *17* (9), 5782-5789.